International Journal of Signal Processing, Image Processing and Pattern Recognition
Vol.9, No.4 (2016), pp.11-26
http://dx.doi.org/10.14257/ijsip.2016.9.4.02

Seam-Based Edge Blending for Multi-Projection Systems

Marius Pedersen[1], Daniel Suazo[1], and Jean-Baptiste Thomas[2]

[1] *Norwegian Colour and Visual Computing Laboratory, Norwegian University of Science and Technology, Gjøvik, Norway*
[2] *Université de Bourgogne, LE2I, UMR CNRS 6306, Dijon, France*
[1]*marius.pedersen@ntnu.no*

Abstract

Perceptual seamlessness of large-scale tiled displays is still a challenge. One way to avoid Bezel effects from contiguous displays is to blend superimposed parts of the image over the edges. This work proposes a new approach for edge blending. It is based on intensity edge blending adapted on the seam description of the image content. The main advantage of this method is to reduce visual artifacts thanks to context adaptation and smooth transitions. We evaluate the quality of the method with a perceptual experiment where it is compared with state-of-the-art methods. The new method shows most improvement in low frequency areas compared to the other techniques. This method can be inserted into any multi-projector system that already applies edge blending.

Keywords*: projector, multi-projector, edge blending, seam carving,luminance mapping*

1. Introduction

Displays that cover a large area represent a consequent application field. From industries and control rooms to entertainment settings, like concerts or art venues through scientific visualisation and gaming, many benefits can be obtained from such displays. However, projectors with resolution capabilities to cover large screen size are prohibitively expensive and technically complicated to handle. They lack flexibility when it comes to adapt to different types of physical environments. A more cost effective solution is the use of multiple projection displays [18, 28, 33, 42, 54, 60, 65], a combination of projectors tiled together to create one large display. Three main applications are usually considered in the literature for multi-display systems: immersive reality (originally for military applications and flight simulation) [14], scientific visualization [58] and collaborative working environment [44, 48, 58]. The major problem to guarantee the seamlessness of the system is geometrical registration. Another issue, to make the user feel like there is only one single display, is photometric and colorimetric spatial uniformity.

Indeed, to project a seamless image we must map a given projector to the surface of the screen for both proper positioning and accurate intensity and color levels. Once these correspondences are made, we can accurately display the union of projectors by correcting for geometric and colorimetric differences. Some books consider exclusively with the technological problems of multi-display systems [8-26].

The technical issues inherent to this technology are listed hereafter:

• Screen properties must be considered in order to reach a better contrast ratio for the whole system. To limit the number of inter-reflections one may use low reflectivity or gray screens [46-50].

• Scalability is important. Adding or removing easily one or several projector(s) is a technical challenge [7, 10, 11].

• Computational complexity and parallel rendering (The capabilities of GPGPU helped a lot to design real time rendering applications) is also a critical aspect [35-66].

ISSN: 2005-4254 IJSIP

Geometry registration and alignment are largely handled with the use of cameras. Methods span from highly calibrated to uncalibrated setups [10, 11, 15, 19].

Color uniformity is considered against different aspects. Intra-projector differences, which consider non-uniformity within a single projector; Inter-projector differences, which consider differences between two projectors; Overlapping areas, which consider part of the image resulting from several projectors overlapping.

Although all aspects must be considered in a practical setup, this work focuses only on the color uniformity aspect, and in particular on the overlapping areas.

A single projector does not reproduce the same color at each different location [2, 21, 30, 49, 55, 56]. This non-uniformity is mainly coming from the fact that the imaging device is decoupled from the screen itself. There is then either a lens effect, or the geometrical arrangement between the projector and the screen that influences this parameter. Different solutions have been proposed in order to have a photometric uniformity. Most consider the use of a camera to set up a luminance attenuation map (LAM), based either on a mathematical model [29-32] or on a look-up-table (LUT) [37, 38]. It is also well understood that several displays produce different colors for a similar input. Then, the input image must be mapped into an output common to all projectors. Beside the physical or manual adjustment possible, such as using the same light bulb, the problem has been addressed mainly by two different means. First, a LAM approach [29-30], that ignores chromatic differences between projectors. Artifacts can be created by such approach [27]. However, this might be reasonable since it has been found that there was a gamut mismatch of only 2.75% between two projectors of the same brand and model with similar time of use [55]. Second, a common gamut has to be found, which is the intersection of all projectors' gamuts involved in the image creation [6, 37, 38, 52, 53, 59]. This method aims at finding the common gamut between all projectors used in the system. Some degree of freedom may be allowed for perceptual gamut homogeneity [47].

In addition to having colorimetric match within a projector and between each projector, a third problem must be addressed. In order to align the images between projectors and suppress the Bezel effect, projectors need to overlap partly in terms of their physical light output. This overlap presents a much brighter area with a visible "hotspot" and an inaccurate color representation. A correction to this problem is usually named edge blending. The edge blending aims at smoothing the overlapping areas between projectors. The literature emphasizes three methods:

• Optical masking [10] modifies the signal (optical or analog) near the border to create a virtual mask for the fusion of images.

• Aperture masking [23] uses physical patterns on the path of the light next to the border of the images.

• Software blending [44] uses a function to attenuate the luminance at the border. This function can be either linear, cosine or S-curve shape.

The two first solutions limit the accuracy of the blending, while the last is limited by the accuracy of the geometric registration. The work presented in this paper focuses on addressing the photometric uniformity in overlapping regions. We propose to use an intelligent software edge blending, where seam carving is used in order to decide how and where to perform blending in order to limit the perception of seam.

This paper is organized as follows: First we present relevant background of edge blending and seam carving. Then we introduce the proposed method. In Section 4 we present the experimental setup, followed by results and discussion in Section 5. At last we conclude and propose future work.

2. Edges in Multi-Display Systems

2.1. Definition of Overlapping Area

For a single projector i, on a given channel l where $l \in \{R, G, B\}$, we consider $C_i(u,v) = T(i,u,v) + T_k(i,u,v)$, where $T(i,u,v)$ represents the colorimetric tristimulus values of the ith projector at the pixel position (u,v) of the input image and $T_k(i,u,v)$ represents the colorimetric tristimulus values of the offset, also called black-level in the literature, of the ith projector at the pixel position (u,v). At the border of the output of one projector, we have the contributions of M projectors overlapping $C(u,v) = \sum_{i=1}^{M}(\mathrm{T(i,u,v)} + \mathrm{T_K(i,u,v)})$.

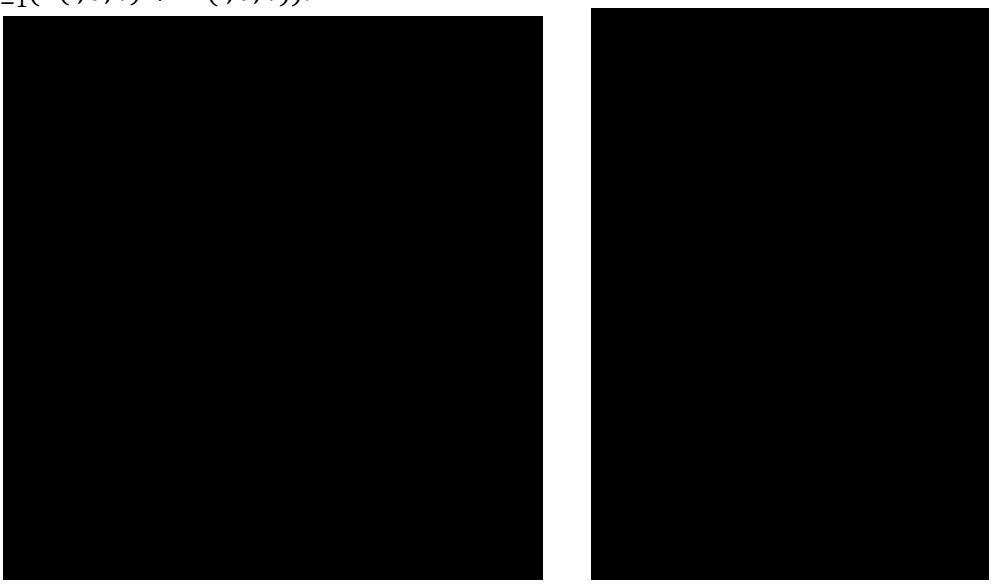

(A)Edge blending (B) Hard seam blending

Figure 1. Comparison between Edge Blending and Hard Seam Blending. Attenuation in Edge Blending Can Be Performed Linearly or Non-Linearly (s-curve for Example)

When we consider now an attenuation mask, we can write the contribution of each projector as $C(u,v) = \sum_{i=1}^{M}(\mathrm{T(i,u,v)} \times \mathrm{A_{i,u,v}} + \mathrm{T_K(i,u,v)})$, where $A_{i,u,v}$ is the attenuation mask value defined for each projector at each location.

It is of major importance to note that the offset of each projector is increasing the offset at the overlapping area as being $O(u,v) = \sum_{i=1}^{M} \mathrm{T_K(i,u,v)}$. This is known to noticeably break seamlessness in darker area.

2.2. Edge Blending

We define edge blending as a mean to blend output at overlapping edges of several video-projection systems in order to ensure a smooth transition between them that does not affect the viewing experience of the user, *i.e.* perceived uniformity. In this case, the attenuation mask $A_{i,u,v}$ is usually a monotonically increasing smooth function from right to left for an image part being in the right. The function is adapted adequately if the image part is in the left, top or bottom.

First implementations of edge blending intended only to reduce the brightness in the overlap area between projectors. They are mostly optical blending techniques, and involve placing physical masks in the optical path of the projectors. This method is still used today [5], and is considered to be effective. The mask creates a gradual attenuation between projectors in the overlapping area, which can be manually adjusted either

mechanically or electronically. Yet, the cost of additional hardware as well as a complicated manual calibration seriously hampers the scalability of the system.

Software edge blending [42][43][9][22][51], which will be referred to solely as edge blending in the rest of this article, creates a mask that smooths the edges by using computer vision techniques. This mask applied to the image to correctly attenuate the light, so that our visual system will not notice the transition, taking advantage of the fact that our visual system is less sensitive to gradual changes. An example of edge blending is shown in Figure 1a. For edge blending to be effective, the size of the mask has to be large enough so that the change in luminance from pixel to pixel is below the just noticeable difference, and therefore cannot be detected by the human eye.

There are several limitations of edge blending. It is very dependent on the size of the overlap area. Since it works with a gradual attenuation, the larger the overlap area being used, the more steps being used for the gradual attenuation, hence, the less apparent the transition will be. A small overlap will often create a stair stepping effect [13]. There could also be a noticeable change in brightness at the fall-off point, where the overlap area ends and only the single projector output is present, particularly due to the presence of a luminance offset. Discontinuities are one quality issue in edge blending [18]. The perceived discontinuity depends also of the attenuation curve used to generate the mask [22]. Furthermore, edge blending methods are often limited in their ability to generate blends of variable overlap [13].

2.3. Edges and Seam Carving

An alternative approach to this problem is to combine projectors where the spatial complexity of the image is sufficiently great to hide any artifacts caused by the overlap. Pedersen and Bakke [41] proposed a method for multi-projector setups based on seam carving. Instead of having a gradual attenuation, a hard edge is placed along an existing edge in the image. This approach is based on the observation that the human visual system is less sensitive at higher frequencies and that the reduction in visibility of a stimulus can be caused by the presence of another stimulus, so called spatial visual masking. In addition, the use of a hard edge means that no constraints on the gamuts may be necessary; therefore the overall brightness is not affected. An example of hard seam blending is shown in Figure 1b. In this case, the attenuation mask $A_{i,u,v}$ is a Heaviside step function centered on the seam for an image part being in the right. The function is adapted adequately if the image part is in the left, top or bottom.

Seam carving [1] was originally proposed as an algorithm for intelligent content-aware resizing of images. The idea behind seam carving is to create an optimal 8-connected path of pixels on a single image from top to bottom, or left to right, where optimality is defined by an image energy function. The energy function can be calculated using gradient magnitude, entropy, or visual saliency for example. Pedersen and Bakke reformulated seam carving as a minimum cost graph cut problem, where the seam is based on the highest amount of energy. This results in having the border between the morphing position at an edge, which should make the transition seamless. The energy function was based on a Sobel edge detection, which was applied to each channel in the RGB colorspace and then summed over the channels. Furthermore, if the color of the image is within the intersection of the two device's gamuts, the visible transition will be less noticeable. Therefore, an additional argument was added to place the seam in areas with a color difference less than 2.3 ΔE_{ab}, which is given by Mahy *et al*. [25] as the just noticeable difference between two colors.

2.3.1. Limitation of Seam Carving: As noticed by Pedersen and Bakke [41], hard edge seam carving is very noticeable in dark uniform areas. This method is only effective for images that have high frequency information in very particular regions, or having an existing hard edge in the overlapping area between the displays. It also has the

disadvantage of having a strongly image dependent performance. Furthermore, the discontinuity created by the luminance offset at the end of one projector will also affect the perceived uniformity.

3. Proposed Method

In this section we present our method for creating perceptually seamless displays. Our approach combines edge blending and seam carving. It has several steps, as presented on Figure 2. In a nutshell, our method looks for a seam, *i.e.* a connected vertical path within the overlapping area, which we follow to apply the blending.

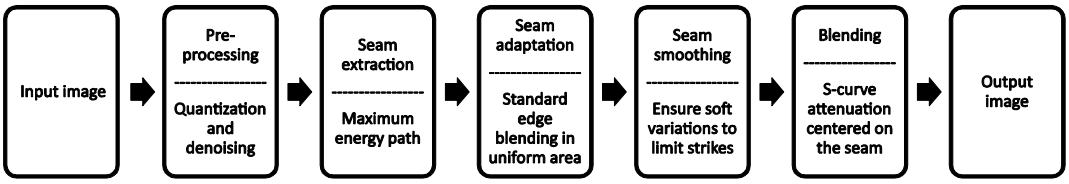

Figure 2. Workflow for the Proposed Seam Based Edge Blending

3.1. Algorithm

From the original image I of size $m \times n$, where m and n is the number of pixels, we define an area in J where the overlap must be present B with size $q \times r$, where q and r is the number of pixels in the overlap area. This area is given by the constraint of the multi-projection system. Then three steps are applied: A pre-processing step, the seam estimation steps, and the blending step as seen in Figure 3.

3.1.1. Pre-Processing: We apply a pre-processing step in order to smooth the flat image content and sharpen major edges. This is simply a denoising-quantization process in order to facilitate the seam extraction.

On each RGB channel a morphological opening is performed with a disk-shaped structural element of four pixels radius. This is done to eliminate irrelevant information and to aid us in grouping together areas that have similar color attributes. Due to the morphological opening, edges become less clearly defined. We thus apply an unsharp masking to the L^* channel of the CIELAB version of the image. This last step emphasizes edges, and the image is ready for seam extraction.

3.1.2. Seam Extraction: To define the seam, we create an energy map based on the gradient of the image on every single channel similar to Avidan and Shamir [1]. We then used the maximum gradient at every pixel position. Given the area of overlap between the projectors in the image I_O, we define a vertical seam as:

$$S^x = \{S_i^x\}^2 = i = 1 = \{(x(i), i)\}_{i=1}^{r}, \text{ s.t. } \forall i, x(i) - x(i-1)| \leq 1, \quad (1)$$

where x is a mapping $x : [1, \ldots, r] \rightarrow [1, \ldots, q]$. This gives a 8-connected path from the top of the image to the bottom with one pixel per row in the image. A horizontal seam can be constructed in a similar fashion.

This energy map can be seen on Figure 3a, and the seam is computed from it. Then, with a given energy function E, we can define the cost of a seam as

$$E(s) = E(J_s) = \sum_{i=1}^{n} e\big(J(s_i)\big), \quad (2)$$

where e is an energy function. In our case we would like to place the seam with maximum energy, *i.e.* we search for the seam s^* that maximizes the following cost function:

$$s^* = \max_s E(s) = \max_s \sum_{i=1}^{n} e\big(J(s_i)\big). \quad (3)$$

In uniform areas of the overlap, uniform edge blending is likely to produce the best result. Therefore, the image is then split in 10 rectangle blocks of equal heights and overlap width. For each block b the standard deviation σ is computed to estimate the variance of the pixel values, as shown in Figure 3. If the standard deviation of a block σ_b is less than a threshold value of 2.2 (a variable value determined by trial and error), there is not a significant amount of variance, therefore uniform edge blending is performed.

A light smoothing is applied between blocks to the seam, in order to avoid sharp varying peaks in the attenuation mask.

3.1.3. Blending: Once the final shape of the mask is determined based on the seam, blending parameters are computed. We used the attenuation S-shape function as defined in Equations 4 and 5, where x is the coordinate of the pixel centered and normalized on the seam, f is the value of the attenuation and p is the parameter that defines the S-shape. For $p = 1$ this curve is a line. We follow the results of Lancelle and Fellner [22] and used $p = 2$.

$$f: \begin{cases} [0,1] \to [0,1] \\ x \to f(x) \end{cases}, \quad (4)$$

such as:

$$\begin{cases} \text{if } x \le 0.5, \ f(x) = \frac{2x^p}{2} \\ \text{else, } f(x) = \frac{2(1-x)^p}{2} \end{cases} \quad (5)$$

A typical mask is shown on Figure 4.

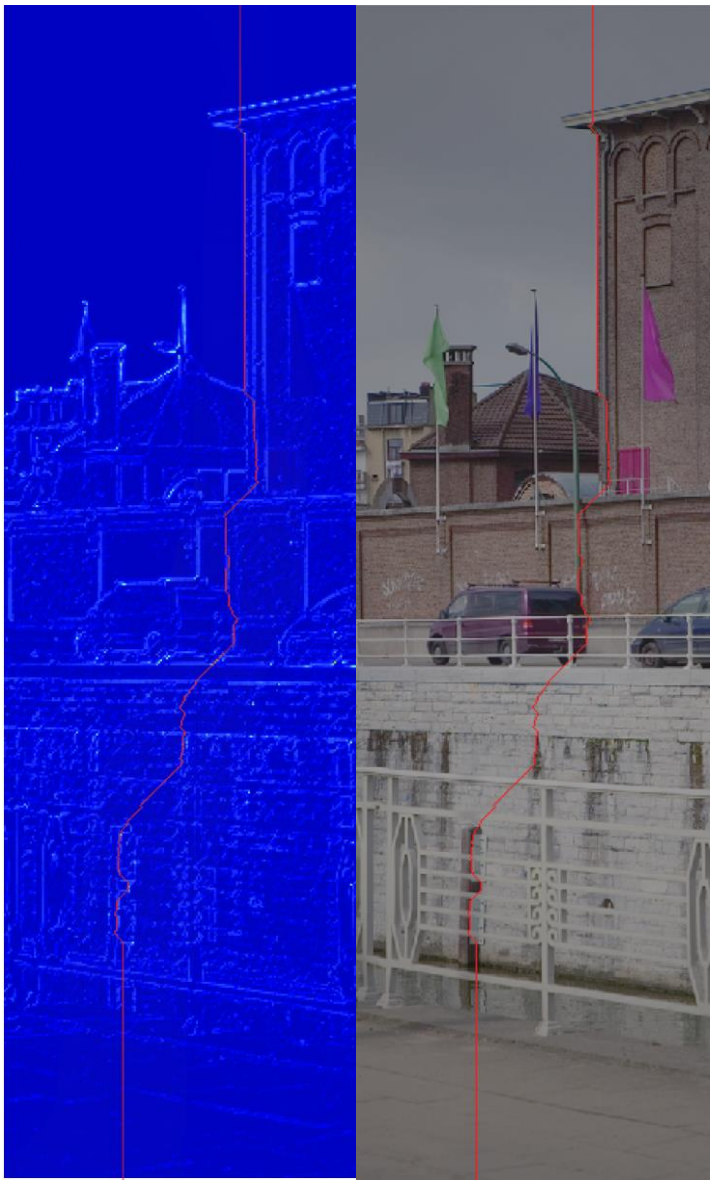

(a)Energy map used to compute the seam (b) Seam overlaying the input image

Figure 3. Figure 3a Shows the Energy Map on Which the Seam Carving is Based. Figure 3b Shows the Seam Overlaying the Input Image. The Red Line Shows the Calculated Seam.

(a) left projector mask (b) right projector mask

Figure 4. Projector Masks. Left and Right Projector Masks for Seam Based Edge Blending

4. Experimental Setup

This section explains how we evaluate the proposed method. The evaluation is first based on the simulation of two different projection systems on one single device in order to allow a simple scalability and changes in parameters. Then, different perceptual evaluation procedures are used, as described in the following.

4.1. Simulation and Dataset

4.1.1. Colorimetric Characterization: We model our projection system in order to control the color it displays. We fix the setup parameters and then use the implementation of the Piece-wise Linear interpolation assuming the Constant Chromaticity coordinates (PLCC) model as written by Thomas *et al*. [57], which includes an offset correction. We measure physical values for primaries at maximum intensity and intensity response curves by channel with a spectroradiometer. This permits to have an objective, and not relative, colorimetric model, which helps in the simulation afterward. The original images are coded in sRGB space. All computations and simulations are done in a colorimetric space afterward, then converted to the projector RGB at the end or sRGB for the online evaluation.

4.1.2. Simulation of a Multi-Projector System: In order to simulate a multi-projection system on one device, we define arbitrary displays with reduced gamuts that fit within the capacity of the real projector. In particular, our simulation accounts for brightness, offset, gamut, dynamic range and spatial luminance uniformity. This simulation does not account for intra-projector chroma spatial non-uniformity. We considered only two displays

vertically tiled. One display is the original one, the second is a virtual one of reduced capacity.

To reduce the capacity of the second simulated display, we use YC_bC_r space and reduce the luminance channel Y by 30% of the real projector output. The color gamut and dynamic range are reduced by performing a color transform based on an ICC profile with a very limited gamut. The selected gamut was based on the MOAB Entrada Rag Natural 1430 UPPPM ICC profile, this was chosen since the white point is more a cream color, resulting in color distortions and significant loss in brightness. This results in a large difference between the gamuts. To simulate the fall off in luminance in both simulated displays, we used a linear luminance attenuation toward the edges.

Lastly a black offset is simulated for each display. Several sources assume that the offset is about 2% of the maximum luminance projected per channel [3, 4, 31, 34]. We thus simulate this by adding 2% of luminance per channel.

4.1.3. Simulation of Blend: The standard software edge blending is applied as defined in Section 3.1.3 on an overlapping area of 20% of each simulated projector. The hard seam is computed within the 20% of overlapping area. The seam based edge blend considers the above seam and allows an attenuation of 10% on each side of the seam. Note that within this setup, the attenuation could go 10% over the overlapping area. This allow the attenuation of both methods to be of the same size, which will not be true in practice but permits a fair evaluation of the blending.

4.1.4. Set of Images: A large image set of 61 images have been selected. The images have been chosen to cover a wide range of characteristics, such as uniform areas, detail level, skin tones, different saturation levels, different hues, *etc*.. Some images originates from the Colourlab Image Database:Image Quality (CID:IQ) [24]. A subset of the images used in the evaluation is shown in Figure 5.

Figure 5. Test Images Used in the Experiment

4.2. Evaluation Methods

Three different types of evaluation is carried out to evaluate the proposed seam based edge blending; qualitative evaluation by the authors, perceptual evaluation by a group of human observers, and objective evaluation using image quality metrics.

4.2.1. Qualitative Evaluation: Visual evaluation is carried out on the large image set containing a total of 61 images. The authors have compared visually the result of the seam

based edge blending and traditional edge blending on each image. Focus is given to artifacts and differences between the two methods.

4.2.2. Perceptual Evaluation: To evaluate the validity of the method, a subjective assessment was performed using QuickEval [36]. Forced-choice paired comparison with flipping of the pairs was chosen as the subjective experimental protocol. The reference image was presented in the middle, and on each side the different reproductions. We compare the proposed seam based edge blending to hard seam blending and traditional edge blending. The experiment was carried out online in uncontrolled conditions. The subjects were instructed to choose the image they preferred, given the reference. Six images (Figure 5), being a subset of the large image set. The number of images follow the recommendations by Keelan and Urabe [20], who recommends a minimum of three images, and CIE [12], who recommends at least four images, and Field [16] who recommends between five and ten images. The images representing particular visual situations of interest were selected from the qualitative evaluation, among them a presentation slide, which is commonly displayed using projectors. A total of 10 observers participated in the experiment, which gives a total of 20 observations per pair.

The data from the perceptual experiment are analyzed statistically using Wilcoxon rank sum test [62] to identify if the medians of the two distributions are equal. This is a non-parametric statistical test that does not assume anything about the probability distribution.

4.1.4. Objective Evaluation: Objective evaluation is done using the Structural SIMilarity (SSIM) metric [61]. This metric has proven to work well for many different quality aspects [39-40] and it is based on comparison of structure, luminance and contrast, being the key attributes for seamlessness blending. We will use the quality maps from SSIM for evaluation of the proposed method. Evaluation with SSIM is done on the large image set containing 61 images, and the images have been converted to grayscale for applying SSIM using the standard Equation 6.

$$I = 0.2989 \times R + 0.5870 \times G + 0.1140 \times B \quad (6)$$

Otherwise, standard parameters for SSIM have been used.

5. Results and Discussion

5.1. Results Qualitative Evaluation

It is well known that our visual system is more sensitive to vertical and horizontal oriented edges compared to oblique oriented edges [17]. Visual investigation of the edge blending method confirms that the vertical edge between two projectors is visually more apparent than the proposed seam based edge blending that can put the edge in other orientations.

Figure 6 shows a close-up of one of the test images. We can see that the proposed seam based edge blending method hides the left edge in the edge between the cloud and the background, and it is therefore no longer perceivable. The right edge is placed with slightly different directions, and becomes less visible compared to traditional edge blending (marked with a red ellipse).

The proposed method performs well in most cases. However, in some images where the edge is changing much horizontally, a ”streaking” effect can be seen. The effect can also be seen in the example projector masks in Figure 4. This artifact only occurs in images with a uniform, or close to uniform, area where the seam is moving back and forth. This effect can, for example, be reduced by changing the standard deviation threshold for the seam or adding a smoothness term that penalizes oscillations in the seam.

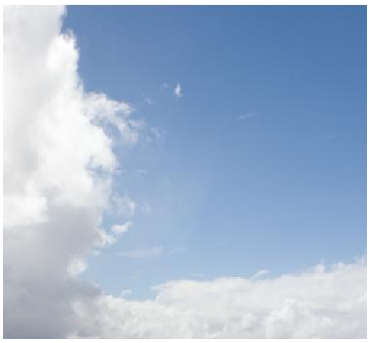

(a) Original

(b) Seam based edge blending

(c) Edge blending

Figure 6. Comparison between the Proposed Seam Based Edge Blending and Normal Edge Blending. The Figure Shows a Cropped Version of a Test Image. A Red Ellipse Highlights the Differences between the Methods, Where the Edge Blending Has a Straight "Line" Going Through the Right Side, and the Same is Not As Visible in the Seam Based Edge Blending.

5.2. Results Perceptual Evaluation

The overall results for the six images from the perceptual experiment can be seen in Table 1. None of the methods have equal medians (as indicated with 1 in Table 1), and the proposed method is statistically significantly better than the edge blending ($p < 0.35e-5$, where p is the probability) and the hard seam ($p < 0.001$). Furthermore, since the performance can be content dependent we have analyzed the results for individual images. The analysis shows that the proposed method is significantly better than the hard seam in all six images. Furthermore, the proposed seam based edge blending method is significantly better than edge blending in two of the six images with a 95% confidence level, for three images the difference is not statistically significantly different with a 95% confidence level, and in the last image edge blending is significantly better with a 95% confidence level.

Table 1. Results from Perceptual Experiment for All Images and Observers. 1 Indicate Different Medians. The Proposed Method is Significantly Better than Edge Blending and Hard Seam Blending.

	Edge blending	Seam based edge blending	Hard seam blending
Edge blending	-	1	1
Seam based edge blending	1	-	1
Hard seam blending	1	1	-

5.3. Results Objective Evaluation

We show representative quality maps from SSIM for a set of images. Figure 7 shows a comparison of the SSIM maps for a part of one image from the seam based edge blending (Figure 7a) and edge blending (Figure 7b). Both maps are shown with the same range. The results from SSIM confirm the visual investigation, and we can clearly see that the left edge is hidden in the seam based edge blending.

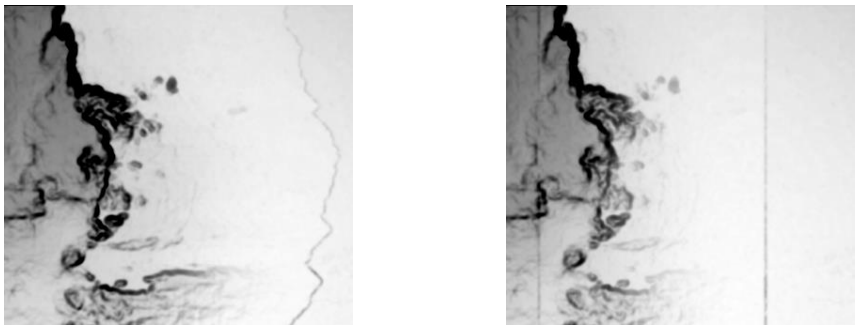

(a) Seam based edge blending (b) Edge blending

Figure 7: Extracted Part from SSIM Maps for the Proposed Seam Based Edge Blending and Edge Blending.

Figure 8 shows another cut out from an image, where edge blending produces a straight line (Figure 8b). This is avoided in the seam based edge blending (Figure 8a). Similar results can be found for other images as well. The streaking artifacts mentioned in Section 5.1 can be easily seen in the SSIM maps (Figure 9).

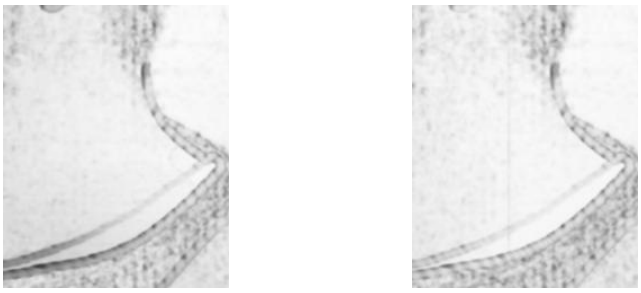

(a) Seam based edge blending (b) Edge blending

Figure 8. Extracted Part of SSIM Maps for the Seam Based Edge Blending and Edge Blending. The Proposed Method Has Placed the Edge Along Content in the Image and Thereby Hiding Transition. The Artifact from Edge Blending is Detected by SSIM in (b), and is a Visible Line.

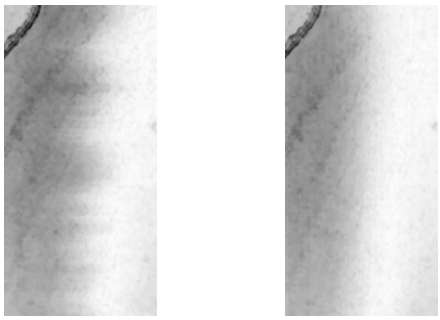

(a) Seam based edge blending (b) Edge blending

Figure 9. SSIM Maps Showing the Streaking Artifacts in the Seam Based Edge Blending Method. The Traditional Edge Blending Method Shows a Smoother Transition without Streaks.

5. Conclusion

The proposed method creates image adapted attenuation maps for projector edge blending and shows promising results. This new method hides the luminance falloff and color distortions in the contours of images. For many cases the resulting blend presents less visual artifacts than edge blending, while preserving the maximum brightness output of each projector. Future works include evaluation of a physical setup with several displays, different orientations and overlapping ratio. Evaluation can also be done using a calibrated digital camera [63-64]. Moreover, investigation to reduce the streaking issues can be investigated. This could be done by a more adapted smoothing process on the mask. Extension of the method to videos using temporal seam carving [45] shall also be considered as it may be a critical counterpart of this method.

Acknowledgements

The authors would like to acknowledge the Color in Informatics and Media Technology Consortium (Universite Jean Monnet, Norwegian University of Science and Technology, Universidad de Granada and Ita-Suomen yliopisto). We would also like to thank Universite de Bourgogne.

References

[1] S. Avidan and A. Shamir, "Seam carving for content-aware image resizing", In ACM Transactions on graphics (TOG), ACM, vol. 26, **(2007)**, pp. 10.
[2] A. M. Bakke, J.-B. Thomas, and J. Gerhardt, "Common assumptions in color characterization of projectors", In Proc. of Gjøvik Color Imaging Symposium, vol. 4 of Proc. of Gjøvik Color Imaging Symposium, **(2009)**, pp. 45–53.
[3] R. Bala and K. Braun, "A camera-based method for calibrating projection color displays", In Fourteenth Color Imaging Conference, Scottsdale, Arizona, USA, IS&T/SID, **(2006),** pp. 148–152.
[4] R. Bala, R. V. Klassen and K. M. Braun, "Efficient and simple methods for display tone-response characterization", Journal of the Society for Information Display, vol. 15, no. 11, **(2007)**, pp. 947–957.
[5] Barco.Barco products @ONLINE, http://www.barco.com/en/Products-Solutions/Options-accessories/Other/Optical-Soft-Edge-Matching.aspx, March **(2014)**.
[6] M. Bern and D. Eppstein, "Optimized color gamuts for tiled displays", In SCG'03: Proceedings of the nineteenth annual symposium on Computational geometry, New York, NY, USA, ACM, **(2003)**, pp. 274–281.
[7] E. S. Bhasker, P.Sinha and A. Majumder, "Asynchronous distributed calibration for scalable and reconfigurable multi-projector displays", IEEE Trans. Vis. Comput. Graph., vol. 12, no. 5, **(2006)**, pp. 1101–1108.
[8] O. Bimber and R. Raskar, "Spatial Augmented Reality: Merging Real and Virtual Worlds", A. K. Peters, Ltd., Natick, MA, USA, **(2005)**.
[9] P. Bourke, "Projector edge blending", **(2014)**, Visited 19/03/15.
[10] C.-J. Chen and M. J. Johnson, "Fundamentals of scalable high-resolution seamlessly tiled projection system", In Ming H. Wu, editor, Projection Displays VII, (SPIE) San Jose, CA, vol. 4294, March **(2001)**, pp. 67–74.
[11] H. Chen, R. Sukthankar, G. Wallace and K. Li, "Scalable alignment of large-format multi-projector displays using camera homography trees", In VIS '02: Proceedings of the conference on Visualization '02, , Washington, DC, USA, IEEE Computer Society, **(2002)**, pp. 339–346.
[12] CIE. Guidelines for the evaluation of gamut mapping algorithms. Technical Report ISBN: 3-901-906-26-6, CIE TC8-03, no. 156, **(2004)**.
[13] R. M. Clodfelter, D. Sadler and Johan Blondelle, "Large high resolution display systems via tiling of projectors", White paper. Barco Simulation Products, **(2002)**.
[14] C.C.-Neira, D. J. Sandin, and T. A. DeFanti, "Surround-screen projection-based virtual reality: The design and implementation of the cave", In Proceedings of the 20th Annual Conference on Computer Graphics and Interactive Techniques, SIGGRAPH '93, New York, NY, USA, ACM, **(1993)**, pp. 135–142.
[15] J. Drareni, S. Roy and P. Sturm, "Geometric video projector autocalibration", In Proceedings of the IEEE International Workshop on Projector-CameraSystems, Miami, Florida, June **(2009)**.
[16] G.G. Field, "Test image design guidelines for color quality evaluation", In 7th Color Imaging Conference, Scottsdale, AZ, November **(1999)**, pp. 194–196.
[17] C. S. Furmanski and S. A. Engel, "An oblique effect in human primary visual cortex", Nat Neurosci, vol. 3, no. 6, June **(2000)**, pp. 535–536.
[18] M. Harville, B. Culbertson, I. Sobel, D. Gelb, A. Fitzhugh and D. Tanguay," Practical methods for geometric and photometric correction of tiled projector", In Computer Vision and Pattern Recognition Workshop, 2006. CVPRW'06. Conference on, IEEE, June **(2006)**, pp. 5.
[19] M. Hereld, I. R. Judson, and R. Stevens, "Dottytoto: a measurement engine for aligning multiprojector display systems", In Ming H. Wu, editor, Projection Displays IX, Santa Clara, CA, SPIE, vol. 5002, January **(2003),** pp. 73–86.
[20] B. W. Keelan and H. Urabe, "A psychophysical image quality measurement standard. In Y. Miyake and D. R. Rasmussen, editors, Image Quality and System Performance, San Jose, CA, ISO 20462, (SPIE), vol. 5294, January **(2004)**, pp.181–189.
[21] Y. Kwak and L. MacDonald, "Characterisation of a desktop LCD projector", Displays, vol. 21, no. 5, **(2000)**, pp.179–194.
[22] M. Lancelle and D. W. Fellner, "Soft edge and soft corner blending", In Work- shop Virtuelle & Erweiterte Realitt (VR/AR), **(2011),** pp. 63–71.
[23] K. Li, H. Chen, Y. Chen, D. W. Clark, P.Cook, St. Damianakis, G. Essl, A. Finkelstein, T. Funkhouser, T. Housel, A. Klein, Z. Liu, E. Praun, R. Samanta, B. Shedd, J. P. Singh, G.Tzanetakis, and J. Zheng, "Building and using a scalable display wall system", IEEE Computer Graphics and Applications, vol. 20, no. 4, **(2000)**, pp. 29–37.
[24] X. Liu, M. Pedersen and J. Yngve Hardeberg, "Image and Signal Processing", 6th International Conference, ICISP 2014, Cherbourg, France, 2014. Proceedings, chapter CID:IQ – A New Image Quality Database,. Springer International Publishing, Cham, June 30 – July 2 **(2014)**, pp.193–202.
[25] M. Mahy, L. V. Van Eycken and A. Oosterlinck, "Evaluation of uniform color spaces developed after the adoption of cielab and cieluv", Color Research & Application, vol. 19, no. 2, **(1994)**, pp. 105–121.

[26] A. Majumder and M. S. Brown, "Practical Multi-projector Display Design", A. K. Peters, Ltd., Natick, MA, USA, **(2007)**.
[27] A. Majumder and M. Gopi, "Modeling color properties of tiled displays", Comput. Graph. Forum, vol. 24, no. 2, **(2005)**, pp. 149–163.
[28] A. Majumder, Z. He, H. Towles and G. Welch, "Achieving color uniformity across multi-projector displays", In Visualization 2000. Proceedings, IEEE, **(2000),** pp. 117–124.
[29] A. Majumder and R. Stevens, "Lam: Luminance attenuation map for photometric uniformity in projection based displays", In Proceedings of ACM Virtual Reality and Software Technology, **(2002)**, pp.147–154.
[30] A. Majumder and R. Stevens, "Color nonuniformity in projection-based displays: Analysis and solutions", IEEE Transactions on Visualization and Computer Graphics, vol. 10, no. 2, **(2004)**, pp.177–188.
[31] A. Majumder and R. Stevens, "Color nonuniformity in projection-based displays: Analysis and solutions. Visualization and Computer Graphics", IEEE Transactions on, vol. 10, no.2, **(2004)**, pp.177–188.
[32] A. Majumder and R. Stevens, "Perceptual photometric seamlessness in projection-based tiled displays", ACM Trans. Graph, vol. 24, no. 1, **(2005)**, pp. 118–139.
[33] B. B. May, N. D. Cahill and M. R. Rosen, "Calibration of a multiprojector system for display on a cylindrical surface", In Image Processing Workshop (WNYIPW), 2010 Western New York, IEEE, **(2010)**, pp. 6–9.
[34] E. B. Mikalsen, J. Y. Hardeberg and J.-B. Thomas, "Verification and extension of a camera-based end-user calibration method for projection displays", In Proceedings of the CGIV 2008/MCS'08 4th European Conference on Colour in Graphics, Imaging, and Vision and 10th International Symposium on Multispectral Colour Science 4,Terrassa, Spain, June **(2008)**, pp. 575–579.
[35] S. Nash and R. Surati, "Using the gpu to create a seamless display from multiple projectors", SIGGRAPH 2011, Presentation, **(2011).**
[36] K. V. Ngo, C. A. Dokkeberg, J. Jr. Storvik, I. Farup, and M.Pedersen, "Quickeval: a web application for subjective image quality assessment,. In Mohamed-Chaker Larabi and Sophie Triantaphillidou, editors, Image Quality and System Performance XII, San Francisco, CA, vol. 9396, Feb. **(2015)**, pp. 9396–24.
[37] A. Pagani and D. Stricker, "Photometric and chromatic calibration for multiprojector tiled displays. In Fourteenth Color Imaging Conference, Scottsdale, Arizona, USA, IS&T/SID, **(2006)**, pp. 291–296.
[38] A. Pagani and D. Stricker, "Spatially uniform colors for projectors and tiled displays", Journal of the Society for Information Display, vol. 15, no. 9, **(2007)**, pp.679–689.
[39] M. Pedersen, "Evaluation of 60 full-reference image quality metrics on the CID:IQ", In International Conference on Image Processing, , Quebec, Canada, IEEE, September **(2015),** pp. 1588 – 1592.
[40] M. Pedersen and J. Y. Hardeberg, "Full-reference image quality metrics: Classification and evaluation. Foundations and Trends in Computer Graphics and Vision", vol. 7, no. 1, **(2012)**, pp.1– 80.
[41] M. Pedersen and A. M. Bakke, "Seam carving for multi-projector displays", **(2011)**.
[42] A. Raij, G. Gill, A. Majumder, H. Towles and H. Fuchs, "Pixelflex2: A comprehensive, automatic, casually-aligned multi-projector display", In IEEE International Workshop on Projector-Camera Systems, Nice, France, **(2003)**, pp.203–211.
[43] R. Raskar, M. S. Brown, R. Yang, W.-C. Chen, G. Welch, Herman Towles, Brent Scales and Henry Fuchs, "Multi-projector displays using camerabased registration. In Visualization'99", Proceedings, San Francisco, CA, USA, IEEE, October **(1999)**, pp.161–522,
[44] R. Raskar, G. Welch, M. Cutts, A.Lake, L. Stesin and H. Fuchs, "The office of the future: A unified approach to image-based modeling and spatially immersive displays", In Proceedings of SIGGRAPH 98, Computer Graphics Proceedings, Annual Conference Series, New York, NY, USA, July **(1998)**, pp. 179–188.
[45] M. Rubinstein, A. Shamir and S. Avidan, "Improved seam carving for video retargeting. ACM Transactions on Graphics (SIGGRAPH)", vol. 27, no. 3, **(2008)**, pp.1–9.
[46] Michael J. Rudd, Patrick M. Dunn and Eric C. Gemmer, "P-237: Measurement of the picture contrast enhancement of gray projection screens", SID Symposium Digest of Technical Papers, vol. 39, no.1, July **(2008)**, pp.2093–2094.
[47] B. Sajadi, M. Lazarov, M. Gopi and A. Majumder, "Color seamlessness in multi-projector displays using constrained gamut morphing", Visualization and Computer Graphics, IEEE Transactions on, vol. 15, no. 6, **(2009)**, pp. 1317–1326.
[48] P. Santos, A. Stork, T. Gierlinger, A. Pagani, B. Araujo, R. Jota, L. Bruno, J. Jorge, J. Madeiras Pereira, M. Witzel, G. Conti, R. Amicis, I. Barandarian, C. Paloc, M. Hafner and D. McIntyre, "Improve: Advanced displays and interaction techniques for collaborative design review", In Randall Shumaker, editor, Virtual Reality, of Lecture Notes in Computer Science, Beijing, China, Springer Berlin Heidelberg, vol. 4563, **(2007)**, pp. 376–385.
[49] L. Seime and J. Y. Hardeberg, "Colorimetric characterization of LCD and DLP projection displays.", Journal of the Society for Information Display, vol. 11, no. 2, **(2003)**, pp. 349–358.
[50] L. P. Skolnick and J. W. Callahan, "Luminance calculation on a spherical projection surface with varying screen gain characteristics", Image VII Conference Proceedings, **(1994)**, pp. 23–32.

[51] Z. Song, G. Gong, Z. Huang, L. Han and Y. Ding, "A new edge blending paradigm for multi-projector tiled display wall. In Computer Application and System Modeling (ICCASM)", International Conference on, Taiyuan, 2010. IEEE, vol. 5, October **(2010),** pp. V5–349 – V5–352.
[52] M. Stone, "Field Guide to Digital Color", A. K. Peters, Ltd., Natick, MA, USA,**(2002)**.
[53] M. C. Stone, "Color and brightness appearance issues in tiled displays", IEEE Comput. Graph. Appl., vol. 21, no. 5, **(2001)**, pp.58–66.
[54] F. Teubl, C. Kurashima, M. Cabral and M. Zuffo, "Fastfusion: A scalable multiprojector system", In Virtual and Augmented Reality (SVR), 201214th Symposium on May **(2012)**, pp. 26–35.
[55] J.-B. Thomas and A. M. Bakke, "A colorimetric study of spatial uniformity in projection displays.",In Lecture Notes in Computer Science, number 5646 in Lecture Notes in Computer Science, Saint-Etienne, France, Springer, **(2009)**, pp. 160–169.
[56] J.-B. Thomas, A. M. Bakke and J. Gerhardt, "Spatial nonuniformity of color features in projection displays: A quantitative analysis", The Journal of imaging science and technology, vol. 54, no. 3, **(2010)**, pp. 030403–13.
[57] J.-B. Thomas, J. Y. Hardeberg, I. Foucherot and P. Gouton, "The plvc display color characterization model revisited", Color Research & Application, vol. 33, no. 6, **(2008)**, pp. 449–460.
[58] G.Wallace, O. J. Anshus, P. Bi, H. Chen, Y. Chen, D. Clark, P. Cook, A.Finkelstein, T.Funkhouser, A. Gupta, M. Hibbs, K. Li, Z. Liu, R. Samanta, R. Sukthankar and O. Troyanskaya, "Tools and applications for large-scale display walls", IEEE Comput. Graph. Appl., vol. 25, no. 4, **(2005)**, pp. 24–33.
[59] G. Wallace, H. Chen and K. Li, "Color gamut matching for tiled display walls", In EGVE '03: Proceedings of the workshop on Virtual environments 2003, New York, NY, USA, ACM, **(2003)**, pp. 293–302.
[60] M. Wang, Y. Han, R. Wang, X. Liu and Y.Qian, "Fpga-based image processing for seamless tiled display system", In Srikanta Patnaik and Xiaolong Li, editors, Proceedings of International Conference on Soft Computing Techniques and Engineering Application,Advances in Intelligent Systems and Computing, Springer, India, vol. 250, **(2014)**, pp. 451–456.
[61] Z. Wang, A. C. Bovik, H. R. Sheikh and E. P. Simoncelli, "Image quality assessment: from error visibility to structural similarity", IEEE Transactions on Image Processing, vol. 13, no. 4, **(2004)**, pp. 600–612.
[62] F. Wilcoxon, "Individual comparisons by ranking methods", Biometrics Bulletin, vol. 1, no. 6, **(1945)**, pp. 80–83,.
[63] P. Zhao, M. Pedersen, J. Y. Hardeberg and J.-B. Thomas, "Measuring the relative image contrast of projection displays", Journal of Imaging Science and Technology, vol. 59, no. 3, **(2015)**, pp. 30404–1–30404–13.
[64] P. Zhao, M. Pedersen, J.-B. Thomas and J. Y. Hardeberg, "Perceptual spatial uniformity assessment of projection displays with a calibrated camera", Color and Imaging Conference, **(2014),** pp. 159–164.
[65] C. Zoido, J Maroto, G. Romero and J. Felez, "Optimized methods for multi-projector display correction", International Journal on Interactive Design and Manufacturing (IJIDeM), vol. 7, no. 1, **(2013)**, pp.13–25.
[66] C. Zoido, J. Maroto, G. Romero and J. Felez, "Optimized methods for multi-projector display correction", International Journal on Interactive Design and Manufacturing (IJIDeM), vol. 7, no. 1, **(2013)**, pp. 13–25.

